

Received 24 November 2023, accepted 15 December 2023, date of publication 18 December 2023, date of current version 26 December 2023.

Digital Object Identifier 10.1109/ACCESS.2023.3344601

## RESEARCH ARTICLE

# Polarization-Insensitive Electromagnetic Metamaterial Design for Multi-Band Energy Harvesting

HUI ZHANG<sup>1</sup>, YANG LI<sup>1</sup>, WENRUI HU<sup>1</sup>, QIBIN LU<sup>1</sup>, BOJUN ZHANG<sup>2,3</sup>, AND LAMAR Y. YANG<sup>4</sup>, (Senior Member, IEEE)

<sup>1</sup>State Key Laboratory of Media Convergence and Communication, Communication University of China, Beijing 100024, China

<sup>2</sup>Shenzhen Academy of Information and Communications Technology, Shenzhen 518048, China

<sup>3</sup>China Telecommunication Technology Laboratories, China Academy of Information and Communications Technology, Beijing 100191, China

<sup>4</sup>Department of Electrical and Computer Engineering, University of Nebraska–Lincoln, Lincoln, NE 68588, USA

Corresponding author: Bojun Zhang (zhangbojun@caict.ac.cn)

This work was supported in part by the National Natural Science Foundation of China under Grant 62101515, Grant 62071436, and Grant U2241229; and in part by the Fundamental Research Funds for the Central Universities.

**ABSTRACT** A multi-band and polarization-insensitive metamaterial is proposed to harvest electromagnetic energy efficiently in three frequency bands. Based on a square resonant ring and cross resonant structure, a metamaterial is designed to achieve high energy harvesting efficiency of 81.2%, 93.3% and 93.5% at 2.45 GHz, 4.0 GHz and 5.8 GHz, respectively. The overall structure consists of an  $8 \times 8$  periodic array of meta-cells with two vias loaded by two  $50 \Omega$  resistors, an impedance matching network and a rectifier circuit. Results show that the simulated rectification efficiency of rectifier circuit reaches 69.2%, 58.8% and 52.1% at 2.45 GHz, 4.0 GHz and 5.8 GHz, respectively, when the incident power is 5 dBm. The measured harvesting efficiency (RF-DC) is found to be 51.6%, 54.2% and 58.7% with the TE polarization and 50.6%, 53.7% and 58.6% with the TM polarization incidence at the three operating frequency bands, respectively. Although the incident power is reduced to 0 dBm, the energy harvesting efficiency can still reach more than 42% in both TE and TM polarizations. Therefore, it is shown that the energy harvesting system can maintain high efficiency under different polarizations in a wide power range.

**INDEX TERMS** Energy harvesting, polarization-insensitive, resonant structure, dielectric substrate, multi-band, rectifier circuit.

## I. INTRODUCTION

With the commercialization of 5G communication technology in more countries, the theory and products of intelligent devices that can collect and process data have received extensive attention in recent years [1], [2], [3]. Low-power intelligent terminals such as various types of Internet of Things (IoT) devices, sensors and implantable medical devices have begun to be widely used in daily life [4], [5], [6]. The power consumption of these small devices has been reduced to the milliwatt level and is widely distributed in various scenarios in our life [7]. Therefore, how to effectively

The associate editor coordinating the review of this manuscript and approving it for publication was Ladislav Matekovits.

capture the incident energy has been a challenge for energy harvesting in low-power applications.

Recently, metasurface absorbers have been exploited for energy harvesting and wireless energy transformation due to their excellent characteristics of managing EM waves. Energy harvesting technology based on metasurface has been widely studied in low-power range. The performance of metasurface is mainly determined by the topological structure and periodic arrangement of its units. Moreover, most of the rectifiers are applied in each metasurface cell. Therefore, the losses of diode used in the rectifier also increases the difficulty of energy capture [8]. This challenge is later solved by drilling vias [9]. The vias connecting the meta-cell to a matching network needs to be located at the area

with the strongest current in the meta-cell to ensure higher collection efficiency. Furthermore, the unit needs to pursue central symmetry [10], [11], [15] to ensure that electromagnetic waves of different polarizations can be captured. However, polarization-insensitive metasurface units in previous research often have four vias and loads [12]. Not only do four vias increase the complexity and manufacturing difficulty of the structure, but it also causes the received electromagnetic energy to be dispersed on multiple loads, which makes it difficult for subsequent power synthesis. Moreover, current studies focus on energy harvesting at broadband [13], [14] and high frequency band [15], but these work bands are not suitable for daily application. Among the recent related research, few designs can simultaneously achieve more than two operating frequency bands, basically working at a single-band [16], [17], [18] and dual-band [19]. In addition, due to the high impedance characteristics of structures such as split ring resonators (SRR) [16], [17], [20], the load resistance used to match some metasurface design is very large. This makes the width of the microstrip line corresponding to large resistance much smaller than the processing precision and it will be quite difficult to match these metasurfaces to the rectifier with  $50 \Omega$  input impedance [18], [21].

In order to solve the above problems, we have referenced some existing works [22], [23], a triple-band and insensitive polarization metasurface with wide incident angle range is proposed for high effective energy harvesting in this letter. The number of vias and resistances in each unit is minimized and  $50 \Omega$  load resistance is used to match meta-cell. To measure the performance of the energy harvesting metasurface, a matching network and a half-wave rectifier circuit are integrated to the metasurface to form an overall energy harvest system.

The letter is arranged as follows. In section II, we propose the metasurface structure design and illustrate its energy harvesting characteristics through simulation. In section III, we designed a rectifier that is consistent with the three-band of the metasurface and explain its rectification performance. In section IV, we tested the energy harvesting system in an anechoic chamber and verified its performance. In section V, conclusions are provided.

## II. METASURFACE ANALYSIS AND DESIGN

### A. METASURFACE CELL GEOMETRY

The three metasurface units presented in this paper are all based on a square resonant ring and cross resonant structures, as shown in Figure 1.

The structure is a typical sandwich structure consisting of two metal layers and a dielectric layer in between. The top metal layer is a resonant structure and the bottom layer is metal ground. In order to minimize the loss of energy, the dielectric with low loss is selected in this design. Thus, Rogers RT6006 is selected, its relative dielectric constant is 6.45 and the loss tangent is 0.0027. Furthermore, copper is used to fabricate the resonant structure, the ground and the

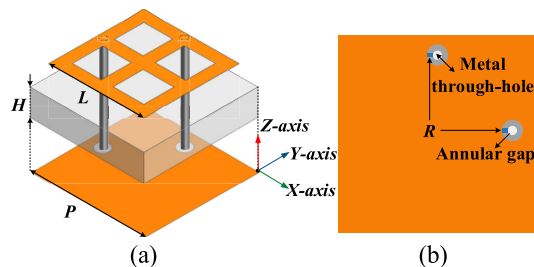


**FIGURE 1.** Configuration of the proposed metasurface unit cell: (a) 3D view of the proposed metasurface unit cell and (b) resistance distribution on the metal substrate. (Where P is the side length of the unit cell, H is the height of the dielectric substrate and L is the side length of the metal resonant structure.)

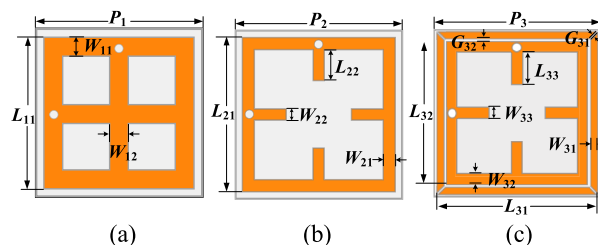


**FIGURE 2.** Metal resonance model: (a) Single-band, (b) Dual-band and (c) Triple-band. (Unit: mm,  $P_1 = 18.3$ ,  $P_2 = 38.8$ ,  $P_3 = 33.5$ ,  $L_{11} = 16.3$ ,  $L_{21} = 36.8$ ,  $L_{22} = 10.9$ ,  $L_{31} = 31$ ,  $L_{32} = 24.5$ ,  $L_{33} = 5.8$ ,  $W_{11} = 2.9$ ,  $W_{12} = 1.9$ ,  $W_{21} = 1.7$ ,  $W_{22} = 4.8$ ,  $W_{31} = 2.2$ ,  $W_{32} = 2.8$ ,  $W_{33} = 2.2$ ,  $G_{31} = 0.6$ ,  $G_{32} = 1.05$ . Particularly, the heights of the three metasurface units are:  $h_1 = 3.7$ ,  $h_2 = 2.1$ ,  $h_3 = 2$ .)

vias. Its conductivity is  $5.8 \times 10^7$  S/m and the thickness is  $35 \mu\text{m}$ .

The resonant structure of the first presented unit cell working at 2.45 GHz is centrosymmetric, which consists of a square resonant ring and a cross resonant structure, as shown in Figure 2(a). Two vias are placed on the two sides of the square ring and two annular gaps are opened around the vias at the ground layer to accommodate the load resistance of  $50 \Omega$ . The top metal patch is connected to the load resistance through a via to ensure that the induced current can be smoothly transmitted to the load when the patch is receiving different polarized incident waves, in order to realize the polarization insensitive characteristics of the metasurface.

Considering the complexity and inconsistency of the ambient electromagnetic environment, multi-band energy harvesting can effectively broaden the application scenarios of the metasurface. The first presented meta-cell is improved to work at 2.45 GHz and 4.0 GHz, so that the metasurface can work in more frequency bands. The second designed meta-cell is shown in Figure 2(b). It also has a typical sandwich structure, but the shape and size of the upper patch were adjusted an opening was designed in the middle of the cross structure to introduce new resonance through the gap, as well.

At present, the most commonly neared Wi-Fi bands are around 2.45 GHz, 4.0 GHz and 5.8 GHz. In order to capture the electromagnetic energy in these frequency bands, we adjusted the geometry and size of the meta-cell and designed a polarization-insensitive metasurface that can work in three frequency bands. Based on the structure of the second

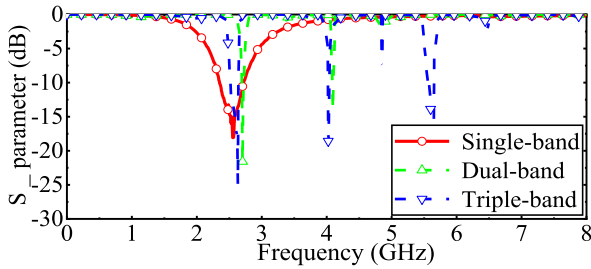


FIGURE 3.  $S_{11}$  parameters of single-band, dual-band and triple-band metasurfaces.

designed meta-cell working in two frequency bands, a square resonant ring with four-corner gaps is added out of the square ring with vias, as shown in Figure 2(c). The gap between the inner and outer square rings can add a new resonance frequency to achieve three operating frequency bands. Furthermore, due to the four gaps of the outer square ring located at its four corners, the maximum induced current of the outer ring appears near the vias of the inner ring. Thus, TE and TM polarization waves in three frequency bands can be received simultaneously without adding new vias in this design. Therefore, the operating frequencies are expanded to three without increasing the complexity of the structure and the difficulty of power combination.

**B. ENERGY COLLECTION PERFORMANCE OF METASURFACES**

To verify the performance of the proposed metasurface, the numerical results were all simulated by using the microwave studio of the commercial simulation software CST. Combined with the periodic boundary conditions and the Floquet port, the metasurface is simulated with an incident plane wave along the  $-z$  direction. The  $S_{11}$  parameters of the three designed metasurfaces are calculated respectively as shown in Figure 3. Since the metasurface unit is a central symmetric structure and is insensitive to polarization, only the simulation results of TE polarization were given. From Figure 3, the  $S_{11}$  parameter of the single-band metasurface can be less than  $-18$  dB at 2.45 GHz. This indicates that the metasurface is well matched with the free space and the reflection of the electromagnetic wave is greatly reduced at 2.45 GHz. The reflection parameters of the dual-band metasurface are lower than  $-20$  dB and  $-13$  dB at 2.45 and 4.0 GHz respectively. Therefore, the values indicate that the metasurface can absorb the incident electro-magnetic energy in two operating bands. The reflection coefficient parameters of the triple-band metasurface at 2.45 GHz, 4.0 GHz and 5.8 GHz are  $-25$  dB,  $-19$  dB and  $-18$  dB, respectively. At these three operating frequencies, the metasurface achieves optimal performance with free space and the electromagnetic wave is nearly not reflected.

To study the energy absorption capacity of the proposed metasurface, the absorption rate can be calculated as follows:

$$A(\omega) = 1 - R(\omega) - T(\omega) \tag{1}$$

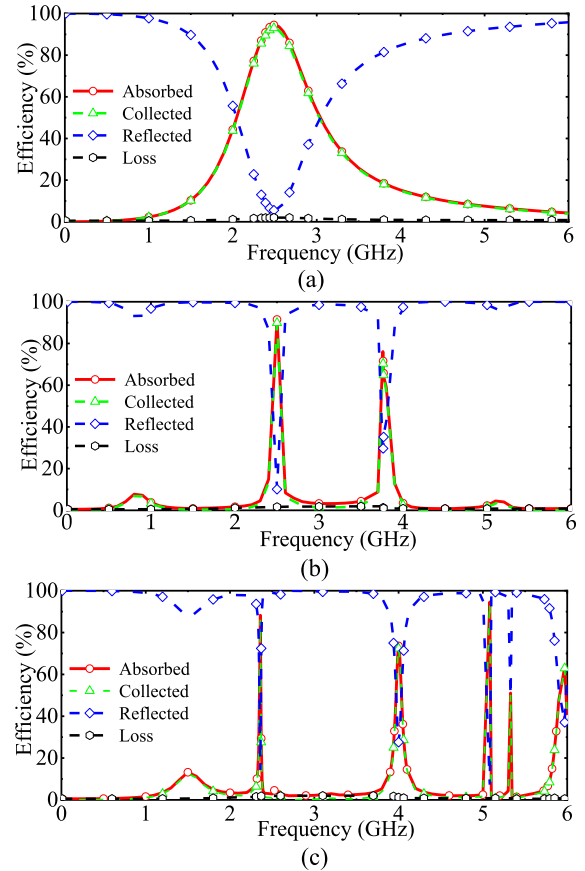


FIGURE 4. Collection efficiency of metasurfaces: (a) single-band, (b) dual-band and (c) triple-band.

where  $A(\omega)$  is the absorptivity of the metasurface,  $R(\omega)$  is the reflectivity and  $T(\omega)$  is the transmittance. Therefore, the absorptivity can be calculated using the  $S$  parameters:

$$A(\omega) = 1 - |S_{11}|^2 - |S_{21}|^2 \tag{2}$$

However, in order to capture and reuse the collection electromagnetic energy, it is not enough to reduce the reflection of electromagnetic waves on the metasurface. It is also necessary to transfer the absorbed electromagnetic energy to the load resistance, so it is better to study the energy transmitting process from free space to the load on the ground. Therefore, the collection efficiency  $\eta_{MS}$  of the energy harvester is defined as:

$$\eta_{MS} = \frac{P_{Load}}{P_{Received}} \tag{3}$$

$P_{Load}$  represents the power absorbed at the load and  $P_{Received}$  represents the power incident into the metasurface. In subsequent studies, the collection efficiency of the metasurface is used to verify its energy capture capacity. It is necessary to note that we directly use the post-processing function of CST to perform formula operations on the obtained data and obtain various results such as absorption efficiency, collection efficiency, reflection efficiency and loss.

Since the metasurface ground is mostly metal, the transmission caused by the circular aperture on the ground is

**TABLE 1. Comparison of proposed work with previous ones.**

Ref.	Overall Size( $\lambda$ L)	Unit	Operating	Load	Energy
		Number	Bandwidths (GHz)	Resistance( $\Omega$ )	Harvesting (%)
[14] (2021)	0.17 $\times$ 0.17 $\times$ 0.139	384	4.3-11	550	85.7%
[16] (2021)	0.15 $\times$ 0.15 $\times$ 0.015	25	2.25	100	90%
[17] (2021)	0.50 $\times$ 0.50 $\times$ 0.041	16	3.75	120	94%
[18] (2022)	0.26 $\times$ 0.26 $\times$ 0.009	64	5.8	50	96%
[22] (2018)	0.08 $\times$ 0.08 $\times$ 0.02	81	2.45	200	92%
[19] (2021)	0.13 $\times$ 0.13 $\times$ 0.010	16	2.45/5.8	70	80%/92%
[23] (2018)	0.22 $\times$ 0.22 $\times$ 0.05	81	2.45/6	240	95%/90%
[20] (2022)	0.23 $\times$ 0.23 $\times$ 0.024	25	2.4/5.2/5.8	377	99%/98%/98% (Without load resistance)
<b>Proposed</b>	<b>0.27<math>\times</math>0.27<math>\times</math>0.016</b>	<b>64(8<math>\times</math>8)</b>	<b>2.45/4.0/5.8</b>	<b>50</b>	<b>81.2%/93.3%/93.5%</b>

almost negligible. Therefore, the energy incident into the metasurface can be divided into the reflected energy and the absorbed energy. The energy absorbed by the metasurface contains two parts, which are the energy collected by the load resistance and the energy lost. The former can be rectified into DC energy and utilized in subsequent work, while the latter is directly consumed in substrate and metal structures, resulting in a decrease in collection efficiency. Thus, in order to ensure the high collection efficiency of the metasurface, it is necessary to minimize the reflection and reduce the energy loss in the substrate.

Based on the above theory, the reflectivity, absorptivity, collection and loss coefficient of incident energy are obtained as shown in Figure 4. In Figure 4 (a), the absorptivity of the incident wave on the single-band metasurface reaches 98.2% at 2.45 GHz from the red curve, the reflected energy is less than 2% of the incident energy from the black curve and the metasurface collection efficiency reaches 93.6% from the green curve. The results indicate that most of the absorbed energy is transferred to the load resistance. Figure 4(b) shows that the dual-band metasurface has a collection efficiency of more than 94% at 2.45 GHz and its collection efficiency reaches more than 93% at 3.8 GHz. In the two operating frequency bands, only less than 6% of the energy decays in the dielectric substrate. The absorption rate of the triple-band metasurface is 99.2% at 2.45 GHz, 99.4% at 4.0 GHz and 98.8% at 5.8 GHz, as shown in Figure 4(c). At 2.45 GHz, the collection efficiency of metasurface was reduced to 81.2% (less than absorptivity) due to part of the energy loss in the medium. While at 4.0 GHz and 5.8GHz, the loss coefficient of the metasurface is less than 7%, the collection efficiency of the metasurfaces is 93.3% and 93.5%, respectively.

The above numerical results show that the metasurface not only has the ability to absorb the incident wave efficiently,

but also most of the absorbed energy is transferred to the load resistance. So, the proposed metasurface has effective energy harvesting performance.

Table 1 lists the comparison between our proposed energy harvesting metasurface and the previous work in terms of overall size, unit number, operating bandwidths, load resistance and energy harvesting. Although, the metasurface unit proposed is relatively small, it works in the three frequency bands with high and stable collection efficiency. Moreover, the load resistance in our design is commonly used in microwave systems.

### C. CHARACTERISTICS OF WIDE INCIDENCE ANGLE AND POLARIZATION INSENSITIVE

Figure 5 shows the collection performance of the metasurface when the electromagnetic wave is obliquely incident at different angles. The incident angle represents the angle between the wave incident direction and the -z direction. It can be observed that when the TE wave is incident, the collection efficiency gradually decreases with the incident angle from 0° to 60°, from 93% to 69% and a certain frequency offset occurs. The maximum frequency offset is about 80 MHz. It can be seen from Figure 5 that the changing trend of the overall collection efficiency when TM wave is incident is almost the same as that of TE wave.

It is shown that the proposed metasurface has both polarization stability and angular stability and can be used for electromagnetic energy harvesting under oblique incidence of different polarized waves from 0° to 60°.

### D. ABSORPTION MECHANISM AND LOAD SELECTION

The working principle of the metasurface is determined by analyzing the surface current distribution at the resonant

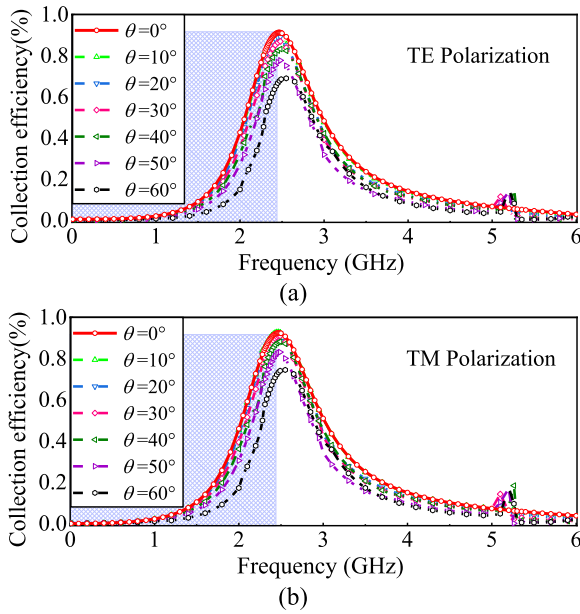


FIGURE 5. The collection efficiency of metasurface under oblique incident electromagnetic waves at different angles: (a) TE polarization and (b) TM polarization.

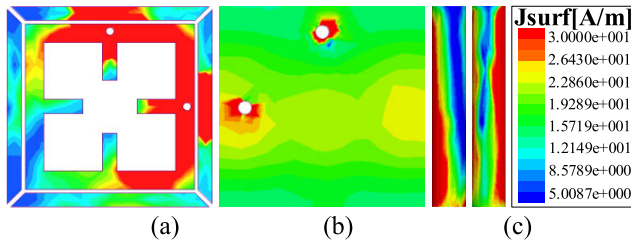


FIGURE 6. Surface current distribution at 2.45 GHz: (a) Metal resonant structure, (b) The metal floor and (c) Metal through-pole.

frequency. The current distribution of the proposed metasurface at 2.45 GHz is calculated in CST as shown in Figure 6.

Clearly, a strong induced current is generated on two square rings and the hollow cross structure at 2.45 GHz. The current is largest near the via and flows along the via to the load.

The function of energy harvesting a metasurface is to achieve matching from free space to terminal equivalent load. The load impedance value will greatly affect the matching between the load and the meta-cell and thus affect the energy capture performance of the metasurface. Therefore, it is necessary to optimize the load resistance value after determining the size, geometric shape and via position of the meta-cell. By adjusting the load resistance, both the collection efficiency and the working frequency band can be significantly changed. Figure 7 shows that the resistance of 50 Ω is already the optimal load for obtaining the efficiency peak for the proposed metasurface working in three frequency bands. Moreover, the load of 50 Ω not only ensures high collection efficiency, but also is a commonly used impedance in the microwave system. Therefore, 50 Ω resistor is selected for subsequent design of the rectifier circuit.

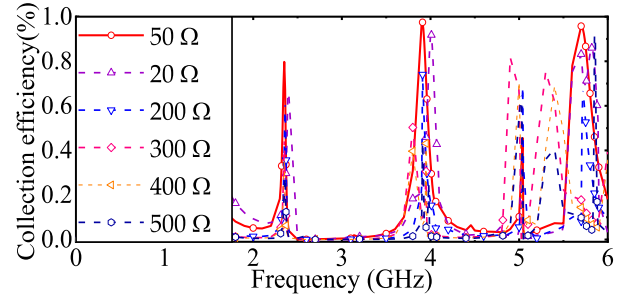


FIGURE 7. The collection efficiency of metasurfaces at different load resistors.

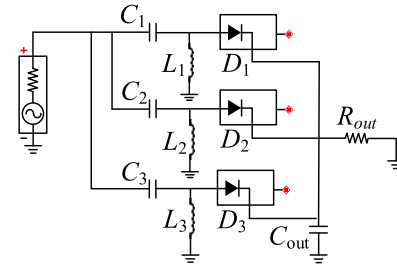


FIGURE 8. The schematic diagram of rectifier circuit. ( $C_1 = 0.5$  pF,  $C_2 = 0.4$  pF,  $C_3 = 0.3$  pF,  $L_1 = 7.8$  nH,  $L_2 = 3.3$  nH,  $L_3 = 1.8$  nH,  $C_{out} = 40$  pF.)

### III. WIDEBAND RECTIFIER CIRCUIT ANALYSIS AND DESIGN

In the electromagnetic energy harvesting system, the rectifier circuit is an important part to determine the energy collection efficiency.

The function of the rectifier circuit is to convert the input AC energy of the rectifier circuit into DC energy. With the aim of obtaining high rectification efficiency under low input power, a rectifier circuit was designed to work at 2.45 GHz, 4.0 GHz and 5.8 GHz.

As Schottky diodes are widely used in the current application, HSMS-2850 is selected as the rectifier diode in our design due to its small conduction voltage, high operating frequency, high conversion efficiency and small volume. Figure 8 shows the schematic diagram of the proposed rectifier circuit.

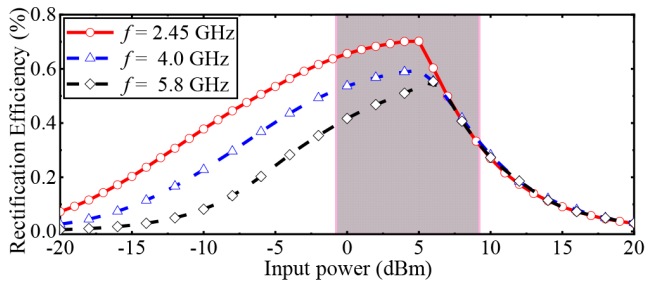
The key indicator to judge the performance of the rectifier circuit is the rectification efficiency, which can be defined as:

$$\eta_{AC} = \frac{P_{Rout}}{P_{AC}} \quad (4)$$

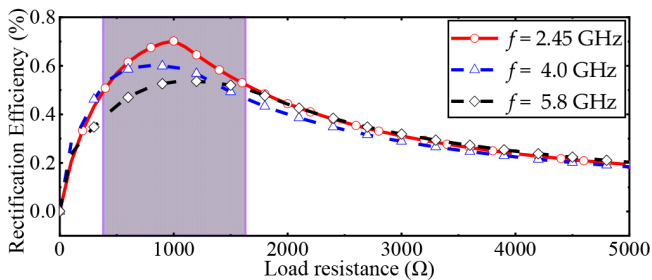
$$P_{Rout} = \frac{V_{Rout}^2}{R_{Rout}} \quad (5)$$

where  $P_{Rout}$  is the power of the load resistance of the rectifier circuit and  $P_{AC}$  is the input power of the transmitter.

The change of rectification efficiency with input power is simulated by using ADS simulation software, as shown in Figure 9(a). It can be seen that when the load resistance is 1000 Ω, the rectification efficiency reaches the maximum of 69.2% with the input power around 5 dBm at 2.45 GHz. Furthermore, the influence of load resistance on the rectification efficiency is obtained by simulation and the results are shown in Figure 9(b). It is indicated that the rectification efficiency



(a)



(b)

**FIGURE 9. The rectification efficiency of the rectifier circuit: (a) Varies with input power at 2.45GHz and (b) Under different load resistance.**

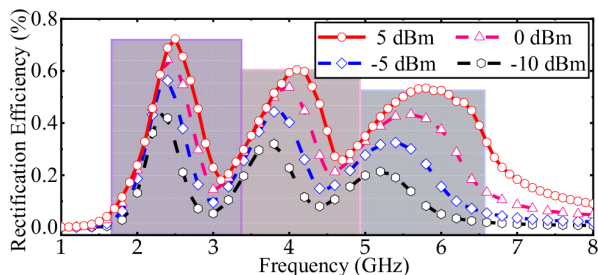


**FIGURE 10. The rectification efficiency changes with frequency under different input power.**

is highest when the resistance reaches around 1000 Ω and the peak efficiencies are above 50% at three frequency points.

Furthermore, the variation of the rectification efficiency with frequency under different input powers is simulated as shown in Figure 10.

We can see that the rectifier circuit has three rectification efficiency peaks at 2.45 GHz, 4.0 GHz and 5.8 GHz, respectively. This is completely consistent with the operating frequency band of the triple-band metasurface designed in this paper.

#### IV. MEASUREMENT AND DISCUSSION

To verify the performance of the designed metasurface, a test system is built in a microwave anechoic chamber, as shown in Figure 11. The proposed metasurface with 8 × 8 cells and the triple-band rectifier circuits were fabricated. Furthermore, a matching network is designed and fabricated on the back of the metasurface to connect the meta-cells and rectifier circuit. Specifically, the energy incident on each meta-cell is collected by the matching network and then transmitted to the rectifier circuit for testing.

To test the sensitivity of the proposed metasurface to input power degree, two input powers, 0 dBm and 5 dBm, are selected to excite the metasurface. The measured efficiency of the energy harvesting system is calculated according to Equation 6-8 [24], [25] and the results are shown in Figure 11.

$$\eta_{\text{Measurement}} = \frac{P_{\text{DC}}}{P_{\text{IN}}} \quad (6)$$

$$P_{\text{DC}} = \frac{V_{\text{out}}^2}{R_{\text{Rout}}} \quad (7)$$

$$P_{\text{IN}} = \frac{G_t \cdot G_a \cdot P}{4\pi R^2} \cdot A_s \quad (8)$$

where  $R_{\text{Rout}}$  is the load resistance at the end of the rectifier, 1000 Ω is selected in this test.  $V_{\text{out}}$  is the DC voltage at both ends of the load,  $G_t$  is the gain of the standard horn antenna,  $G_a$  is the gain of the power amplifier,  $P$  is the input power generated by the signal generator,  $R$  is the distance between the horn antenna and the metasurface and  $A_s$  is the effective acceptance area of metasurface [26].

Figure 12 shows that the frequency points of the measured efficiency peaks are 2.48 GHz, 4.08 GHz and 5.09 GHz, respectively, which have about 0.08 GHz offset from the simulation results. In this work, the  $xoz$  plane is the incident plane. TE polarization refers to the incident wave with an electric field that is perpendicular to the incident plane, while the magnetic field of TM polarization wave is perpendicular to the incident plane.

When the power of TE incident wave is set to be 5 dBm, the measured efficiency of the metasurface reaches 51.6%, 54.2% and 58.7% in three frequency bands, respectively. And the measured efficiency of the metasurface with 5 dBm TM wave incidence reaches 50.6%, 53.7% and 58.6% in three frequency bands, respectively. All efficiency peaks are maintained above 50% under 5 dBm input power. When the input power is reduced to 0 dBm, despite a slight decrease in the measured efficiency, the energy harvesting system can still work properly. When the metasurface is excited by TE polarized wave, the measured efficiency at three frequency points is 42.4%, 45.5% and 47.2%, respectively. Under TM polarization, the measured efficiencies are 42.5%, 44.8% and 49.0%, respectively. Therefore, the proposed metasurface can be used for low-power and Arbitrary-polarization electromagnetic energy collection.

Based on the similar work studied on the triple-bands, we compared the measured efficiency (RF-DC) with the results of [20]. Under TE polarization, the measured efficiency reaches 60% only at 2.45 GHz in [20] and is below 40% at 4.0 and 5.8 GHz. However, the measured efficiency of our metasurface remains above 50% in all three frequency bands and can be close to 60% at most. Especially at 4.0 and 5.8 GHz, it can still maintain a high conversion efficiency. The measured results show that the operating frequency of the energy harvesting system based on metasurface is consistent with the simulation results and the high conversion efficiency can be maintained at low input power regardless of TE wave or TM wave incidence.

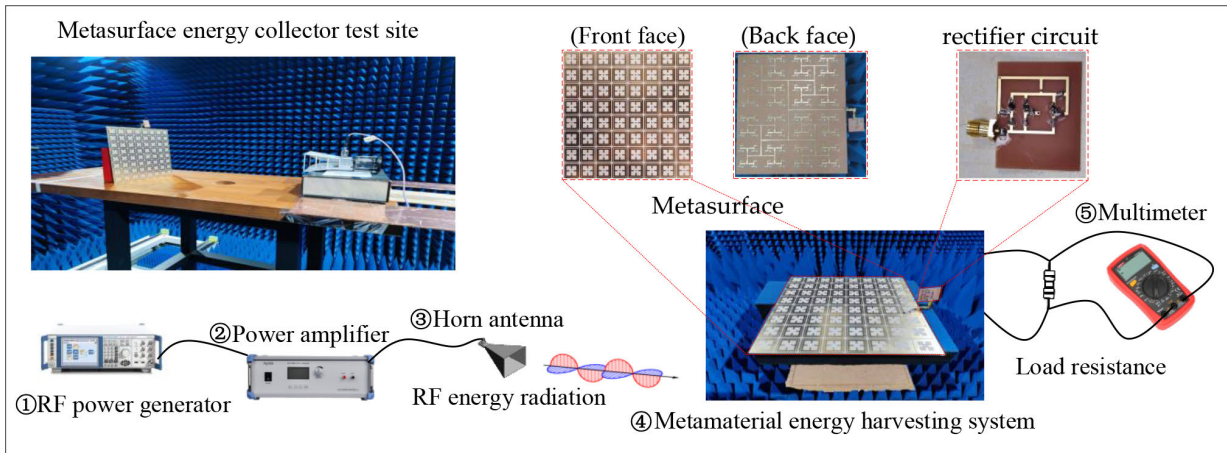


FIGURE 11. Experimental environment and setup of the proposed wireless power transfer system.

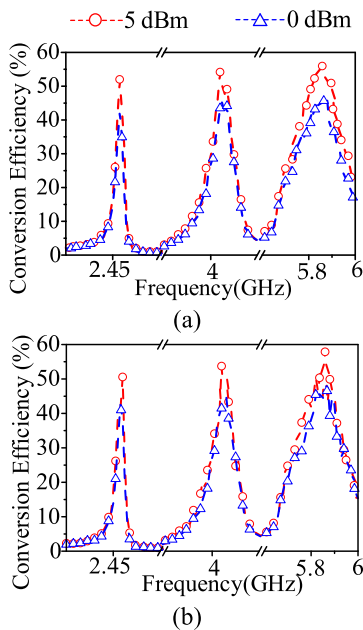


FIGURE 12. The measured conversion efficiency: (a) TE polarization and (b) TM polarization.

V. CONCLUSION

A multi-band polarization-insensitive electromagnetic metasurface was designed and analyzed for energy harvesting. The proposed structure adopts a central symmetrical structure, which can simultaneously capture TE polarized and TM polarized waves. The simulated results showed that the collection efficiency peak achieved by the prototype is over 82% at 2.45 GHz and over 93% at 4.0 and 5.8 GHz. Moreover, this structure has high angular stability, regardless of TE or TM polarization and the designed metasurface unit only has two vias and loads. The load resistance used in the metasurface is 50 Ω, which is commonly used in RF circuits. Moreover, a rectifier circuit was designed with three frequency points. Experimental results show that the energy harvesting system based on metasurface can achieve high RF-DC conversion efficiency. The proposed metasurface realizes

the advantages of multi-band, high efficiency, oblique polarization and wide incidence angle, which is very suitable for wireless power supply of miniaturized terminal equipment in IoT applications.

ACKNOWLEDGMENT

The authors would like to thank Zully Mora Sierra, a Staff of the University of Nebraska–Lincoln, for proofreading.

REFERENCES

- [1] B. Strassner and K. Chang, “Microwave power transmission: Historical milestones and system components,” *Proc. IEEE*, vol. 101, no. 6, pp. 1379–1396, Jun. 2013, doi: 10.1109/JPROC.2013.2246132.
- [2] M. Song, P. Belov, and P. Kapitanova, “Wireless power transfer inspired by the modern trends in electromagnetics,” *Appl. Phys. Rev.*, vol. 4, no. 2, Jun. 2017, Art. no. 021102.
- [3] K. Tutuncuoglu, “Energy harvesting wireless networks: Transmission policies and coding schemes,” Pennsylvania State Univ., State College, PA, USA, Tech. Rep., 2015.
- [4] X. Kong, Y. Wu, H. Wang, and F. Xia, “Edge computing for Internet of Everything: A survey,” *IEEE Internet Things J.*, vol. 9, no. 23, pp. 23472–23485, Dec. 2022, doi: 10.1109/JIOT.2022.3200431.
- [5] D. Vergnaud, “Comment on ‘efficient and secure outsourcing scheme for RSA decryption in Internet of Things,’” *IEEE Internet Things J.*, vol. 7, no. 11, pp. 11327–11329, Nov. 2020, doi: 10.1109/JIOT.2020.3004346.
- [6] D. Jing, H. Li, X. Ding, W. Shao, and S. Xiao, “Compact and broadband circularly polarized implantable antenna for wireless implantable medical devices,” *IEEE Antennas Wireless Propag. Lett.*, vol. 22, no. 6, pp. 1236–1240, Jan. 2023, doi: 10.1109/LAWP.2023.3237558.
- [7] D. H. Nguyen and J. Khazaei, “Unified distributed control of battery storage with various primary control in power systems,” *IEEE Trans. Sustain. Energy*, vol. 12, no. 4, pp. 2332–2341, Oct. 2021, doi: 10.1109/TSTE.2021.3091976.
- [8] D. Ferreira, L. Sismeiro, A. Ferreira, R. F. S. Caldeirinha, T. R. Fernandes, and I. Cuiñas, “Hybrid FSS and rectenna design for wireless power harvesting,” *IEEE Trans. Antennas Propag. Lett.*, vol. 64, no. 5, pp. 2038–2042, May 2016, doi: 10.1109/TAP.2016.2536168.
- [9] T. S. Almoncef, F. Erkmen, and O. M. Ramahi, “Harvesting the energy of multi-polarized electromagnetic waves,” *Sci. Rep.*, vol. 7, no. 1, p. 14, Nov. 2017.
- [10] J. Liu, J.-Y. Li, and S.-G. Zhou, “Polarization conversion metamaterial surface with staggered-arrangement structure for broadband radar cross section reduction,” *IEEE Antennas Wireless Propag. Lett.*, vol. 18, no. 5, pp. 871–875, May 2019, doi: 10.1109/LAWP.2019.2904547.
- [11] M. R. Nickpay, M. Danaie, and A. Shahzadi, “A wideband and polarization-insensitive graphene-based metamaterial absorber,” *Superlattices Microstructures*, vol. 150, Feb. 2021, Art. no. 106786.

- [12] H.-T. Zhong, X.-X. Yang, C. Tan, and K. Yu, "Triple-band polarization-insensitive and wide-angle metamaterial array for electromagnetic energy harvesting," *Appl. Phys. Lett.*, vol. 109, no. 25, Dec. 2016, Art. no. 253904.
- [13] T. Jang, H. Youn, Y. J. Shin, and L. J. Guo, "Transparent and flexible polarization-independent microwave broadband absorber," *ACS Photon.*, vol. 1, no. 3, pp. 279–284, Mar. 2014.
- [14] H. Jiang, W. Yang, R. Li, S. Lei, B. Chen, H. Hu, and Z. Zhao, "A conformal metamaterial-based optically transparent microwave absorber with high angular stability," *IEEE Antennas Wireless Propag. Lett.*, vol. 20, no. 8, pp. 1399–1403, Aug. 2021, doi: [10.1109/LAWP.2021.3081620](https://doi.org/10.1109/LAWP.2021.3081620).
- [15] S. Hannan, M. T. Islam, A. F. Almutairi, and M. R. I. Faruque, "Wide bandwidth angle- and polarization-insensitive symmetric metamaterial absorber for X and Ku band applications," *Sci. Rep.*, vol. 10, no. 1, p. 10338, Jun. 2020.
- [16] M. Amin, T. S. Almomneef, O. Siddiqui, M. A. Aldhaeabi, and J. Mouine, "An interference-based quadruple-L cross metasurface absorber for RF energy harvesting," *IEEE Antennas Wireless Propag. Lett.*, vol. 20, no. 10, pp. 2043–2047, Oct. 2021, doi: [10.1109/LAWP.2021.3102494](https://doi.org/10.1109/LAWP.2021.3102494).
- [17] M. Dinh, N. Ha-Van, N. T. Tung, and M. Thuy Le, "Dual-polarized wide-angle energy harvester for self-powered IoT devices," *IEEE Access*, vol. 9, pp. 103376–103384, 2021, doi: [10.1109/ACCESS.2021.3098983](https://doi.org/10.1109/ACCESS.2021.3098983).
- [18] C. Wang, J. Zhang, S. Bai, X. Zhu, and Z. Zheng, "A harmonic suppression energy collection metasurface insensitive to load and input power for microwave power transmission," *IEEE Trans. Microw. Theory Techn.*, vol. 70, no. 8, pp. 4036–4044, Aug. 2022, doi: [10.1109/TMTT.2022.3182238](https://doi.org/10.1109/TMTT.2022.3182238).
- [19] L. Li, X. Zhang, C. Song, W. Zhang, T. Jia, and Y. Huang, "Compact dual-band, wide-angle, polarization-angle-Independent rectifying metasurface for ambient energy harvesting and wireless power transfer," *IEEE Trans. Microw. Theory Techn.*, vol. 69, no. 3, pp. 1518–1528, Mar. 2021, doi: [10.1109/TMTT.2020.3040962](https://doi.org/10.1109/TMTT.2020.3040962).
- [20] Y. Wei, J. Duan, H. Jing, Z. Lyu, J. Hao, Z. Qu, J. Wang, and B. Zhang, "A multiband, polarization-controlled metasurface absorber for electromagnetic energy harvesting and wireless power transfer," *IEEE Trans. Microw. Theory Techn.*, vol. 70, no. 5, pp. 2861–2871, May 2022, doi: [10.1109/TMTT.2022.3155718](https://doi.org/10.1109/TMTT.2022.3155718).
- [21] F. Yu, X. Yang, H. Zhong, C. Chu, and S. Gao, "Polarization-insensitive wide-angle-reception metasurface with simplified structure for harvesting electromagnetic energy," *Appl. Phys. Lett.*, vol. 113, no. 12, Sep. 2018, Art. no. 123903.
- [22] B. Ghaderi, V. Nayyeri, M. Soleimani, and O. M. Ramahi, "Multi-polarisation electromagnetic energy harvesting with high efficiency," *IET Microw. Antennas Propag.*, vol. 12, no. 15, pp. 2271–2275, Dec. 2018.
- [23] B. Ghaderi, V. Nayyeri, M. Soleimani, and O. M. Ramahi, "Pixelated metasurface for dual-band and multi-polarization electromagnetic energy harvesting," *Sci. Rep.*, vol. 8, no. 1, Sep. 2018, Art. no. 13227.
- [24] F. Erkmen, T. S. Almomneef, and O. M. Ramahi, "Scalable electromagnetic energy harvesting using frequency-selective surfaces," *IEEE Trans. Microw. Theory Techn.*, vol. 66, no. 5, pp. 2433–2441, May 2018, doi: [10.1109/TMTT.2018.2804956](https://doi.org/10.1109/TMTT.2018.2804956).
- [25] C. Song, Y. Huang, P. Carter, J. Zhou, S. D. Joseph, and G. Li, "Novel compact and broadband frequency-selectable rectennas for a wide input-power and load impedance range," *IEEE Trans. Antennas Propag.*, vol. 66, no. 7, pp. 3306–3316, Jul. 2018, doi: [10.1109/TAP.2018.2826568](https://doi.org/10.1109/TAP.2018.2826568).
- [26] F. Erkmen and O. M. Ramahi, "A scalable, dual-polarized absorber surface for electromagnetic energy harvesting and wireless power transfer," *IEEE Trans. Microw. Theory Techn.*, vol. 69, no. 9, pp. 4021–4028, Sep. 2021, doi: [10.1109/TMTT.2021.3087622](https://doi.org/10.1109/TMTT.2021.3087622).



**YANG LI** is currently pursuing the degree with the School of Information and Communication Engineering, Communication University of China. Her current research interest includes analysis and design of metasurface-based wireless power transfer systems.



**WENRUI HU** received the B.Eng. and M.S. degrees in electromagnetic field and microwave technology from the Communication University of China, Beijing, China, in 2017 and 2020, respectively. His current research interest includes analysis and design of metasurface-based wireless power transfer systems.



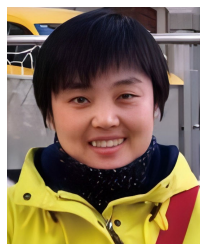
**QIBIN LU** received the degree from the Broadcasting Institute, Department of Electronic Engineering, Beijing, in 2000. He is currently a Master's Supervisor with the Communication University of China. His research interests include digital communication technology, radio frequency technology, and audio technology.



**BOJUN ZHANG** is currently the Vice President of the China Academy of Information and Communications Technology (Shenzhen Academy of Information and Communications Technology), Southern Branch. His research interest include the Internet of Things, electromagnetic compatibility, electromagnetic radiation, electromagnetic field and microwave, and related technology research.



**LAMAR Y. YANG** (Senior Member, IEEE) received the B.S. degree in electrical engineering from Northern Jiaotong University, China, the M.S. degree in electrical engineering from the Beijing Broadcast Institute, China, and the Ph.D. degree in wireless communications and networks from the University of Texas (UT) at Austin, in 2006. He is currently an Associate Professor with the Department of Computer and Electronics Engineering, University of Nebraska–Lincoln (UNL).



**HUI ZHANG** received the Ph.D. degree in communication and information system from Beijing Jiaotong University, Beijing, China, in 2009. She is currently a Professor with the Communication University of China, Beijing. Her research interests include finite-difference time-domain (FDTD) methods, electromagnetic scattering, and microstrip antenna arrays.